Early *C. elegans* embryos modulate cell division timing to compensate for, and survive, the discordant conditions of a severe temperature gradient

Eric Terry[1,2], Bilge Birsoy[1], David Bothman[2], Marin Sigurdson[2], Pradeep M. Joshi[1], Carl Meinhart[2], and Joel H. Rothman[1,*]

1. Department of MCD Biology and Neuroscience Research Institute, University of California Santa Barbara, CA, USA 93106

2. Department of Mechanical Engineering, University of California Santa Barbara, CA, USA 93106

*Corresponding author: Joel H. Rothman

Email: joel.rothman@lifesci.ucsb.edu

Abstract

Despite a constant barrage of intrinsic and environmental noise, embryogenesis is remarkably reliable, suggesting the existence of systems that ensure faithful execution of this complex process. We report that early *C. elegans* embryos, which normally show a highly reproducible lineage and cellular geometry, can compensate for deviations imposed by the discordant conditions of a steep temperature gradient generated in a microfluidic device starting at the two-cell stage. Embryos can survive a gradient of up to 7.5°C across the 50-micron axis through at least three rounds of division. This response is orientation-dependent: survival is higher when the normally faster-dividing anterior daughter of the zygote, AB, but not its sister, the posterior P_1, is warmer. We find that temperature-dependent cellular division rates in the early embryo can be effectively modeled by a modification of the Arrhenius equation. Further, both cells respond to the gradient by dramatically reducing division rates compared to the predicted rates for the temperature experienced by the cell even though the temperature extremes are well within the range for normal development. This finding suggests that embryos may sense discordance and slow development in response. We found that in the cohort of surviving embryos, the cell on the warmer side at the two-cell stage shows a greater average decrease in expected division rate than that on the cooler side, thereby preserving the normal cellular geometry of the embryo under the discordant conditions. A diminished average slow-down response correlated with lethality, presumably owing to disruption of normal division order and developmental fidelity. Remarkably, some inviable embryos in which the canonical division order was reversed nonetheless proceeded through relatively normal morphogenesis, suggesting a subsequent compensation mechanism

46 independent of cell division control. These findings provide evidence for a previously
47 unrecognized process in *C. elegans* embryos that may serve to compensate for
48 deviations imposed by aberrant environmental conditions, thereby resulting in a high-
49 fidelity output.

50

51

Introduction

The development of a complex multicellular animal from a zygote requires coordination of diverse biological processes. Each step in the process is associated with a particular rate of error and is subject to perturbation by genetic variation, environmental fluctuations, and intrinsic molecular noise [1]. Nonetheless, despite the incessant onslaught of error-provoking influences, development generally proceeds faithfully in organisms spanning metazoan phylogeny [2–8]. The observed rate of success is remarkable: throughout the complex process of embryogenesis, cells must properly satisfy many parameters of identity and behavior, including appropriate gene expression, incidence and timing of cell division, and spatiotemporal positioning. This ability of development to proceed with high fidelity in the face of environmental and intrinsic variation likely reflects evolutionary selection for robustness-conferring cellular and molecular mechanisms [1].

While the processes that regulate spatiotemporal developmental fidelity have not been comprehensively elucidated, several mechanisms that influence developmental precision have been uncovered. The molecular chaperone, Hsp90, has been found to act as a buffer against cryptic variation in both fly and vertebrate models [9–14], helping to ensure appropriate cellular identity during development. Robustness in spatial coordination is exemplified by transformation of a variable Bicoid gradient along the antero-posterior axis of the *Drosophila* embryo into spatially stereotyped expression pattern of hunchback and ultimately cellular identity along the anterior-posterior axis of developing embryos [3,15,16]. In vertebrates, Notch directs intercellular temporal coordination and precision during somite development [17] and mutations in the Notch

signaling pathway result in the loss of the normal synchrony in division oscillations of somite cells [17–19]. While such findings shed light on processes that regulate developmental precision, systems that mediate developmental fidelity, particularly in the temporal dimension, are not well understood.

The early cell divisions in *C. elegans* embryos establish six "founder cell" lineages. While the founder cells are born by a series of asynchronous divisions, all their descendants divide in approximate synchrony with a cell cycle periodicity that is unique to that lineage [20]. Although the different founder cell division clocks are not synchronized with each other, they must be kept in precise register to ensure the highly stereotyped arrangement of cells that is characteristic of early embryogenesis [20,21]. This reproducible geometry is critical for signaling events that depend on the proper spatial arrangements of cell-cell contacts that are essential for normal development to proceed [22,23].

The differential apportionment of cell division clocks is evident as early as the two-cell stage, in which the larger, anterior daughter of the zygote, the AB blastomere, divides before its posterior sister, P_1, with high precision. This difference in cell cycle timing is passed onto the descendants of each cell, such that the cell cycle periodicity in the AB lineage is shorter than in the P_1 lineage. The regulation of this differential timing control system has been thought to be determined by cell-autonomous mechanisms; when isolated AB and P_1 are allowed to develop in culture, the relative division timing difference is largely preserved [20,24–28]. The difference in the cell cycle clocks of AB and P_1 largely correlates with their different molecular content and size [25,29,30], which are controlled

by the machinery that establishes anteroposterior polarity in the zygote following fertilization [31–33].

The high fidelity of molecular processes such as DNA replication and aminoacyl-tRNA charging [34,35] result from reactions that correct errors after they are made and it is conceivable that errors made in embryogenesis are often corrected through subsequent developmental processes. Indeed, development is characterized by substantial plasticity and regulatory mechanisms often generate precise patterning from more disordered assemblages of cells (e.g. ordered patterning of hair follicles [36] and robust patterning by morphogen gradients [37–43]). When cells in different domains of *Drosophila* embryos are forced to develop at different rates by imposition of a temperature (T) gradient, abnormal patterns of cell divisions arise (with fewer nuclei on the colder side); however, developmental gene expression is resolved into normal patterns along the axis [44,45], revealing that the gene expression patterning machinery can correct for abnormal cellular patterns that were induced by discordant conditions occurring earlier in development.

The highly stereotypical division sequence and arrangement of early blastomeres in the rapidly developing *C. elegans* embryo [20,21,24,46,47] persists across developmental rates that vary over nearly an order of magnitude (dependent on the T of the environment), providing a useful system for probing mechanisms that ensure developmental precision and fidelity. How are the founder cell lineages, each with different cell cycle clocks, coordinated irrespective of developmental rate, environmental variation, and intrinsic molecular noise, ensuring a reproducible outcome? It is conceivable that communication between cells in different lineages functions to tune cell

120 division timings while they are occurring, thereby continuously maintaining proper
121 harmony across the developing embryo. Alternatively, deviations might be compensated
122 by subsequent error-correcting responses that renormalizes cellular geometry.

123 If early *C. elegans* embryos harbor mechanisms that correct for environmental
124 variation, then they may undergo stereotypical development even under the discordant
125 conditions imposed by a T gradient that, in the absence of such correction, would drive
126 cell divisions and placements to deviate from the normal pattern.

127 In this study, we investigated whether developing *C. elegans* embryos can
128 compensate and correct for discordant conditions between lineages by subjecting them
129 to steep T gradients along the long (anteroposterior) axis. To achieve this, we designed,
130 fabricated, and validated a novel microfluidic device that establishes a steep T gradient
131 in which the two extremes are nonetheless within the permissive T ranges for normal
132 development. While embryos in this steep gradient would be predicted to undergo out-of-
133 sequence division patterns and die in the absence of correction, remarkably, we found
134 that embryos can survive a T gradient of up to 7.5˚C across the 50-micron axis through
135 at least three rounds of division from first cleavage, suggesting that they can compensate
136 for the large discordance imposed by the gradient. This response showed orientation-
137 dependence: survival was higher when the normally faster-dividing anterior daughter of
138 the zygote, AB, but not its posterior sister, P_1, was at the warmer T. We found that the
139 division timing of both AB and P_1 slowed down dramatically in the presence of the gradient
140 compared to the predicted rates, suggesting that embryos may sense and respond to the
141 “crisis” of a discordant condition by activating a checkpoint-like system. Further, cells on
142 the warmer side slow by a larger extent relative to predicted rates than cells on the cooler

side, with the result that the normal division sequence and geometry are preserved. The magnitude of this response correlated with embryo survival: those with a stronger "tuning" response (adjustment in division rate) showed a higher tendency to survive, whereas those with a modest response generally died, suggesting that the response ensures normal developmental progression. In the largest T gradient, the canonical division sequence of many embryos was reversed, with a warmer P_1 dividing ahead of AB. Although such embryos invariably died, some nonetheless showed signs of relatively normal morphogenesis, suggesting a later compensation mechanism can act independently of cell division control. These findings are consistent with the possibility that early *C. elegans* embryos possess mechanisms that sense and correct for noise-induced variation at the time it occurs and respond by adjusting cell division rates to restore the normal pattern of development.

Results

Development and validation of a microfluidics T gradient device

We sought to investigate whether early *C. elegans* embryos are capable of responding to, and correcting for, severely discordant environmental conditions by subjecting them to a steep T gradient across their long axis. We posit that if no compensation system exists, this environmental discordance would drive opposite ends of the embryo to develop at different rates. Based on the known relationship between development timing and T[48], a gradient of 5°C across the 50 µm anteroposterior axis would be expected to create an ~1.5x difference in the developmental rates of P_1 and AB in the absence of any adjustments made by the embryo. To perform this test for developmental compensation, we designed and fabricated a microfluidic device (Fig. 1; Movie S1; see Materials and Methods) that establishes a gradient of up to 7.5°C across the long axis of the developing embryo, while ensuring that the cells within the embryo remained within permissive, non-stressful Ts for normal development (between 16˚C and 24˚C).

The microfabricated device that generated the T gradient used a platinum Joule micro-heater to establish the high T side of the gradient and a chilled fluid mixture to cool the surface opposite from that containing the heater. The magnitude of the T gradient was controlled by varying the T of the cooling fluid and the power through the Joule heater. Embryos were flowed into the device through microchannels with a syringe pump and properly oriented and trapped between pillars in the microfluidic device (Fig. 1E, F; Movie S2).

Computational model and numerical simulations predicted that the device would effectively generate the desired magnitude of T gradient. We experimentally validated the actual T profile of the device by filling the microchannels through which embryos were delivered with a T-dependent fluorophore, dextran-conjugated rhodamine B (DCRB), and measuring the relative quantum yield (Fig. 2B, C). The measured T profile closely matched that of the modeled distribution (Fig. 2B, D). We modeled heat transfer through the eggshell and cytoplasm to assess whether the T gradient experienced by the embryo is likely to diverge substantially from the measured environment in the channel (see Materials and Methods). Using even extremely conservative parameters, neither the eggshell, nor fluid convection, reduce the T-gradient in the embryo by more than a few percent, hence the device effectively generates a pole-to-pole difference in T experienced by the embryo of up to 7.5°C.

Embryonic survival is dependent on orientation and magnitude of the T gradient

C. elegans embryos develop successfully over a broad T range of 6°C to 26°C. At uniform T, the rate of development and cell division increases by ~50% for every 5°C increase in T [48]. If cells in a T gradient divide at the rate predicted from the average T experienced and the embryo is unable to correct for this discordance, the division sequence would be expected to diverge substantially from the normal pattern. At the two-cell stage, for example, this could reverse the normal division order, in which the AB cell divides before the P_1 cell. Such out-of-sequence divisions would be expected to result in aberrant arrangements of cells that diverge substantially from the normally highly stereotyped pattern. Given the rapid intercellular signaling events in the early embryo that are essential for normal cell specification and position [22,29,32,33,49,50] and that

depend upon precise alignment of signaling and receiving cells, such derangement of the pattern would be expected to lead to defective embryogenesis, as evidenced by a failure to hatch. Thus, we asked whether discordance imposed by the steep T gradient results in aberrant cell division and geometry and consequent lethality.

We performed an initial assessment to determine whether 1-4-cell stage embryos can survive in a T gradient by loading them into an early version of the device in which the magnitude of the T gradient differed depending on the position of the captured embryo in the device (Fig. 3). This approach allowed us to evaluate hatching as a function of different gradient magnitudes without changing experimental parameters. A flow rate of at least 25 nl/min was essential for adequate oxygen and CO_2 exchange required to keep embryos viable in the microfluidic device even in absence of a gradient (Fig. 3A). The embryos were subjected to an optimal flow rate of 500 nl/min, which is 20x the critical flow rate necessary for viability without altering the T gradient profile of the microfluidic device (see supplemental text). Early embryos were subjected to the T gradient for ~1 hour, unloaded from the device, allowed to develop, and scored the following day for hatching on culture plates. We found that the embryos were frequently able to survive through to hatching into viable L1 larvae after exposure to the gradient during the crucial early periods of development. The survival (hatching) rate showed an approximately monotonic decrease with increasing magnitude of the gradient (Fig. 3B). While all embryos survived exposure to a 2°C gradient (n=9), ~50% survived in a pole-to-pole T gradient of 2.5-3°C (n=20) and ~25% survived as the magnitude of the gradient was increased from 3°C to 5.5°C (n=46). Under these conditions, none of the embryos exposed to a 6°C T differential hatched (n=5). These initial observations revealed that a)

early exposure of *C. elegans* embryos to a T gradient results in significant lethality, b) the degree of lethality correlates with the magnitude of the gradient, and c) some embryos can survive even in very substantial gradient of ~5.5°C along the long axis.

To observe individual divisions and characterize the survival of one and two-cell embryos subjected to the gradient as a function of number of divisions, we loaded embryos into a modified device before the division of the first cell, and after the division of the first cell. This allowed us to measure the times of division for each cell while in the gradient. Embryos were loaded into the device in either orientation such that, for some, AB was on the warmer end of the gradient (positioned toward the heater), and for others, P_1 was warmer. Embryos were allowed to develop in the gradient through the division of the daughters of AB and P_1, unloaded, allowed to develop at constant T, and scored for hatching ~24 hours later. Confirming the results with the earlier device, we found that embryos were frequently able to survive a large T gradient (Fig. 3C). The hatching rate of embryos subjected to the gradient starting at the two-cell stage again correlated roughly monotonically with magnitude of the T gradient. Remarkably, we found that some embryos were able survive a very steep pole-to-pole gradient of 7°C.

We observed that the ability of early embryos to survive exposure to the gradient was orientation-dependent. Embryos that were placed in the gradient such that AB was warmer than P_1 showed a statistically significantly higher (65.8%; n=38) rate of hatching when compared to embryos with the opposite orientation (P_1 warmer than AB) (28.6% n=42; p=0.0015 Fisher exact test). Above the threshold of a 5°C gradient, survivability in both orientations started to drop, with P_1 warmer embryos experiencing a significantly larger drop in survival (Fig. 3C). At the highest magnitude of gradient (7°C), while nearly

246 a quarter of the embryos survived when AB was oriented toward the warm end of the
247 gradient (n=18), all embryos (n=17) in the reverse orientation died, a significant difference
248 (p=0.045). These results raise the possibility that the more rapidly dividing AB cell can
249 more effectively "tune" its division rate in response to discordance than the slower dividing
250 P_1 cell, consistent with our observations of cell cycle timing adjustment (see below).

251 **Early rates of division described with a modified Arrhenius equation**

252 We sought to test the possibility that the ability of embryos to survive a T gradient
253 might reflect a system that monitors deviations in the early cell division and then adjusts
254 cell division timings to normalize these deviations. To do so, it was necessary to quantify
255 the T-dependent behavior of the cells at uniform constant Ts, and assess whether cells
256 divide at rates that differ from those predicted for their T environment under the discordant
257 conditions of the gradient. If the two-cell *C. elegans* embryo adjusts cell division timings
258 based on this discordance, this effect would be revealed as a tendency for one or both of
259 the cells to divide at a rate other than that expected for the T experienced by that cell. To
260 reveal any such an effect, it was necessary to measure the division rates for AB and P_1
261 at a range of constant Ts, and build a quantitative mathematical model of the division time
262 for the second and third divisions in the AB and P_1 lineages as a function of T (Fig. 4A &
263 B).

264 We found that the T-dependent times of division for both cells in the two-cell
265 embryo measured at progressively increasing constant T are empirically closely
266 described by a modified Arrhenius equation. This finding is consistent with those
267 described by Begasse et al. [51] for T-dependent rates of pre-division events observed in
268 the one-cell P0 zygote in both *C. elegans* and *C. briggsae*. In that study, as in ours, the

data was modeled by performing a least-squares fit to a linearized version of the Arrhenius equation in which the log of the rate (or time interval) of an event is evaluated as a function of the reciprocal of T at which the rate (or time to division) was measured. However, and significantly, our model differs from the previous work in at least one important aspect. The earlier work [51] used the absolute T scale of Kelvin to describe the relationship between rate and T. While this is consistent with calculation of T-dependent chemical rates using the Arrhenius equation, it makes the assumption that the event under consideration progresses at some rate down to a T approaching absolute zero. However, such an assumption does not hold for typical biological processes. In an alternative method introduced by Nakamura et al. [52], an additional T term is introduced into the denominator of the independent variable of the linear form of the Arrhenius equation, allowing for greater empirical fitting of data:

$$ln(\Gamma_1 - \Gamma_0) = B(\frac{1}{T-T_0}) + ln\, A$$

This additional term, which acts as an offset for the measured T of the data, can be thought of as the T at which of the rate for the system under consideration extrapolates to zero. We sought an estimate for this T for *C. elegans* by performing two methods of analysis on our data: a numerical-simulation-generated general non-linear fit of the data, performed in Comsol Multiphysics, and a parametric sweep of this offset T on the linear model of the data. Both methods were in high agreement (~one part in 100 difference) and revealed that the offset T that best fits our data for the N2 strain of *C. elegans* for the second and third division of the embryo is -10˚C. This parameter implies a *C. elegans*-specific “absolute zero” T, at which all cellular activity stops, a more biologically relevant assumption.

Embryos respond to a T gradient by slowing overall developmental rate

Our modified Arrhenius equation allowed us to calculate an expected rate of cell division at any T within the experimental T ranges and to assess whether the individual cells divided at a rate consistent with, or deviating from, the local T that they experience in the gradient. We followed cell division microscopically throughout exposure to the gradient and quantified the temporal division behavior of each of the cells in the two-cell embryo. This analysis revealed two striking trends in the quantitative behavior of the individual cells within the gradient (Fig. 4C-H).

First, we found that the timing of cell divisions in the gradient showed much greater variability than that observed for embryos at constant T. To compare the variance of cohorts of embryos across the various conditions, we calculated the coefficient of variation (CV) for each cohort of embryos at each of the constant Ts, as well as the CV of each cohort of embryos that experienced the same T gradient magnitude and orientation. The mean coefficient of variation across constant Ts for both AB and P_1 were 0.10, and the standard deviation of the CVs across the different constant Ts were 0.05 and 0.04 respectively. The mean CV of the various cohorts of embryos experiencing the T gradient was 0.19 and 0.18 for AB and P_1 respectively with a standard deviation of CVs across gradients and orientations of 0.06 and 0.04 for AB and P_1 respectively. That the standard deviation of the CVs stayed relatively constant across both constant Ts and T gradient conditions and orientations, while the magnitude of the CV doubled for the various T gradient conditions when compare to the constant T divisions, implies that the presence in the gradient imposes greater variability in division timing.

Second, we found that the division rates of both cells, independent of the orientation of the embryos in the gradient, decrease in the T gradient relative to their expected T-dependent behavior at their local T. This effect suggests that embryos respond to the discordant conditions by reducing the overall rate of development. Regardless of the mechanism underlying this process, many embryos showing this greatly reduced developmental rate survived, revealing their ability to adjust to these highly aberrant conditions (Fig. 3 and see below). There were two exceptions to the general trend of slowing relative to the rate expected for T environment. First, for embryos that experienced a T gradient of 5°C starting at the 1-cell stage, the division rates were more consistent with the expected behavior for the local T (Fig. 4I and J). Moreover, the rate of division of P_1 in embryos exposed to the largest gradient (Fig. 4H) similarly deviated less dramatically from the expected behavior. In both cases, embryos in the cohorts that tracked more closely with expected timing were much more likely to die, a trend that we observed more generally as well (see below).

On average, the warmer cell slows more than the cooler cell in viable embryos irrespective of orientation

While imposition of the T gradient slowed the division rate of both AB and P_1, it was possible that a compensation process that normalizes the division sequence might occur in which one cell is subject to greater reduction in division rate than the other, depending on orientation in the gradient. To assess the extent to which the cell division rate was altered, we analyzed the division timing of each cell (AB and P_1) relative to the other. For each embryo analyzed, we determined the fold change in division timing for

each of the cells of the two-cell embryo by calculating the $\log_2$ of the ratio of observed and expected time of division at the average T experienced by each cell. The behavior of each embryo was then graphed as a single point, with the behavior of AB plotted on the x axis and P_1 on the y axis (Fig. 5). This treatment allowed us to simultaneously identify how each cell behaved relative to both its expected behavior and to that of the other cell, as explained in Fig. 5A. The results allowed us to compare the deviations in developmental timing of each cell relative to the other in the context of the entire embryo with those measured in embryos developing at constant T. Consistent with the high fidelity of early *C. elegans* development, we found that embryos at constant T showed low variation in cell division rates around the origin of both axes [$\log_2$ (expected: observed) = ~0]. If division timings of both cells slowed by the same magnitude relative their expected timings, the results would fall on a line with slope = 1, and the distance from the origin along this line would reflect the overall slow-down as a result of the gradient. Divergence from this line indicates that the division rate of one of the two cells deviated from the expected division rate by a larger extent than the other cell.

The data were partitioned into four groups. Results for embryos in each orientation (AB warmer *vs.* P_1 warmer) were averaged and plotted separately. Further, to assess whether the degree of deviation in cell division timing might correlate with successful embryogenesis in the discordant conditions, the results were further separated based on the ultimate outcome (viability *vs.* lethality) following exposure to the gradient.

This analysis revealed a striking outcome: embryos that developed and hatched (i.e., were viable) showed a substantially larger average overall reduction in division timing from that expected at constant T (greater distance from the origin) compared to the

cohort of embryos that failed to hatch (i.e., were lethal) (Fig. 5C). Thus, survival correlated with greater slow-down in division rates of both AB and P_1, irrespective of orientation in the gradient.

For the cohort of embryos that survived, we found that the two cells showed a pronounced orientation-dependent difference. For viable embryos positioned in the gradient with P_1 on the warmer end, the slow-down in average division rate from the expected rate was greater for P_1 than for AB. Similarly, viable embryos in which AB experienced the warmer environment showed a greater reduction in average division rate of AB compared to P_1 (Fig. 5C).These results suggest that, for surviving embryos, while the division of both cells slowed dramatically in the T gradient, the cell on the warmer side tended to respond to the discordance to a greater degree relative to the T it experienced than that on the cooler side, with the outcome that normal division sequence was preserved.

We observed a second orientation-dependent effect: viable embryos in which P_1 was warmer(P_{1warm}) than AB experienced a greater magnitude in slowdown of P_1 relative to the extent of slowdown of AB in the viable AB_{warm} embryos . Regardless, in both cases, the cell on the warmer side of the gradient always showed greater deviation from the expected rate. AB, the faster dividing cell under normal conditions, appears to be more effective at responding to the discordance than P_1, the normally slower developing cell, a finding that is consistent with the orientation-dependent effect on lethality described above (Fig. 5C).

In contrast to the results with viable embryos, the cohorts of inviable embryos tended to show a substantially reduced average response of both AB and P_1: in both

384 orientations, the data clustered closer to the origin than for the viable embryos. Moreover,
385 unlike the surviving embryos, these inviable embryos showed a greater reduction in
386 division rate of AB compared to P_1 in *both* orientations, with the result that the data for
387 the two orientations clustered together (Fig. 5C).

388 In summary, we found that both AB and P_1 greatly reduce their division rates in
389 embryos that survive the T gradient and that the cell that would be expected to divide
390 more rapidly on the basis of its higher T environment shows a larger response (greater
391 reduction in division rate) than its cooler neighbor.

392

393 **Evidence for a later compensation mechanism: morphogenesis can progress**
394 **despite reversal in the AB and P_1 division sequence**

395 Under the most extreme conditions, we found that the T gradient was sufficient to
396 force reversal of the stereotyped division sequence of AB and P_1 (Fig. 6). For embryos
397 subjected to the gradient after cleavage of P0 and oriented with P_1 on the warmer side,
398 we found that a steep T gradient was sufficient to reverse the normal division sequence
399 and drive P_1 to divide before AB in 60% (9/15) of embryos subjected to a 6.5°C gradient,
400 and 71% (12/15) of those experiencing a 7°C gradient. Further, initiation of the gradient
401 prior to the division of P_0, in which the posterior side of the embryo was oriented toward
402 the warmer end of gradient, resulted in reversal of the division sequence in 90% (9/10) of
403 the embryos. As expected, none of these embryos in which the sequence of division was
404 reversed survived and hatched. Unexpectedly, however, a substantial fraction of such
405 embryos proceeded through relatively normal morphogenesis: 32% (9/28) of embryos
406 that experienced a reversal in division sequence of AB and P_1 gave rise to an arrested

407 embryo that appeared relatively normal in morphology and had undergone substantially
408 normal morphogenesis (Fig. 6). Moreover, we found that 43% (6/14) of lethal embryos
409 that experienced any of the gradients in which AB was warmer than P_1, similarly
410 proceeded through relatively normal morphogenesis. These findings revealed that even
411 under extremely discordant conditions that drive complete reversal of the stereotyped
412 division sequence in the very early embryo, later embryos appear to be capable of
413 compensating sufficiently well that morphogenesis, if not fully successful development,
414 can occur. These observations underscore the substantial ability of *C. elegans* to correct
415 for aberrations in cell division and placement patterns.
416

Discussion

A largely unexplored problem in animal biology is how complex developmental processes result in a reliable output in spite of constant environmental and intrinsic noise. Our goal in this study was to test whether animal embryos that normally show a highly stereotyped pattern of development are capable of responding to, and correcting for, the discordant conditions imposed by a T gradient. We propose that this discordance is a proxy for natural noise that embryos normally experience which, in the absence of any correction, might otherwise cause them to deviate from the stereotypical pattern. These studies demonstrated that *C. elegans* embryos both respond to a T gradient and can adjust division timings to generate a normal pattern of development despite highly discordant T's.

In this study, we report the following major findings. 1) We have designed, fabricated, and validated a microfluidics device that effectively establishes a steep T gradient of up to 7.5°C across the 50 µm anteroposterior axis of *C. elegans* embryos. 2) We have characterized the division time of the two-cell embryo as a function of T and established a mathematical model describing the relationship. 3) Embryos through at least the second round of division can survive exposure to a pole-to-pole gradient of up to 7°C and hatch into viable larvae. 4) Survival in the T gradient is orientation-dependent: embryos in which AB is positioned on the warmer side can withstand a larger gradient than those in the reverse orientation. 5) Embryos exposed to the T gradient slow their average developmental rate dramatically compared to those embryos that do not survive to hatching at the same gradient magnitude. 6) While the rate of division of both cells at the two-cell stage is reduced in the gradient, the cell on the warmer end shows a tendency

441 to slow by a larger degree than that on the cooler end, thereby often preserving the normal
442 geometry of the embryo. 7) Survival correlates with the magnitude of this cell division
443 response: the cohort of embryos that died showed a lower average deviation in division
444 timing from that predicted based on their T environment. 8) Some embryos in which the
445 AB/P_1 division sequence was reversed invariably died but nonetheless showed signs of
446 relatively normal morphogenesis, suggesting the existence of later developmental
447 compensation mechanisms.
448
449 **Evidence for multiple compensation/correction systems in embryos**
450 Mechanisms that detect and correct for "errors" resulting from noisy development
451 processes might function by (A) sensing deviations in rates or timing of events outside
452 normal bounds and adjusting for these deviations at the time of their occurrence, or (B)
453 by acting at pre-established stages (perhaps "checkpoints") to detect aberrant events that
454 have occurred in the past, and make repairs through subsequent compensation
455 processes. Our findings are consistent with both types of systems in *C. elegans* embryos.
456 The finding that the division of both cells slows in the gradient relative to the
457 expected behavior is consistent with the possibility that the discrepancy from normal
458 development imposed by the gradient activates a checkpoint-like system in which a
459 "crisis" leads to slowing or pausing of the cell cycle (as occurs, for example, in genotoxic-
460 induced stress [29,53–55]. This effect correlates with survival: the cohort of embryos that
461 survived showed the most dramatic reduction in developmental rate. We postulate two
462 possible explanations for this effect. First, it is conceivable that T gradient across each
463 cell induces a cell-intrinsic process that slows the rate of division in response to the

464 aberrant environment independently of effects on the other cell. A second possibility is
465 that such a response might result from intercellular communication between AB and P_1
466 that instructs both cells to slow or “wait” until adjustments to division rates have been
467 made. In such an event, this cell-extrinsic communication would be bidirectional, as both
468 cells slow down relative to their expected behaviors. Thus, each cell at this, and possible
469 later stages, might compare its progress with neighboring cells and “tune” its division
470 timing in such a way that the proper geometry is ensured. Resolution of these alternatives
471 would require creating a step-gradient in which two sharply delineated T’s are imposed
472 upon the cells, where each T is experienced uniformly across the full dimension of the
473 cell. If the effect we have observed also occurs under such conditions, it would strongly
474 argue that the effect is mediated through cell-extrinsic signaling.

475 We found that as early as the two-cell stage, embryos show evidence of “tuning”
476 of cell divisions in response to deviations: under conditions in which each cell would be
477 expected to divide at an inappropriate time relative to the other, AB and P_1 often appear
478 to adjust their division rates in a way that maintains their normal relative division
479 sequence. It is therefore conceivable that a cell that might be driven to divide more rapidly
480 as a result of a warmer T might alter its division rate based on information about the rate
481 of its cooler neighbor. Our results suggest that when its cooler neighbor is lagging, AB
482 shows a greater capability for slowing its division than does P_1. This is reflected both in
483 the magnitude of the division rate decrease (Fig. 5) and the higher viability of embryos in
484 which AB is located on the warm side than those in reverse orientation. Given that AB is
485 the “leader” during normal development (i.e., it divides before P_1 under constant T
486 conditions), this may reflect the intrinsic ability of AB under normal conditions to monitor

and respond to its slower neighbor as needed to maintain the proper relative division timing. Regardless, if AB and P_1 undergo intercellular communication to regulate developmental progress, it could explain the observation that isolated AB blastomeres, obtained by removal of P_1 by extrusion from the eggshell or through isolation in culture, undergo slower rates of division ([27,56,57]; our unpublished observations); in the absence of information from P_1 that might indicate progress in its development, AB may default to a slower division rate. Our findings also raise the question of whether the adjustment in cell division timing observed here is related to a different cell timing compensation mechanism: the negative correlation between cycle timing of a cell and its descendant, in which cells that divide early give rise to granddaughters that are more likely to divide late [46].

Our observations suggest that the capacity of embryos to compensate for the discordance of the T gradient can be exceeded beyond an acceptable “dynamic range” under extreme conditions. Most or all embryos fail to complete normal embryogenesis when exposed to the largest gradient (Figs. 3 and 5). We note that under these extreme conditions, the magnitude of the overall slowdown relative to the expected rate is less than under milder T gradient conditions, suggesting that the response system may be overwhelmed by this environment. It is also striking that the cohort of surviving embryos show the greatest average reduction in both overall cell division rate and in relative slowdown of the warmer vs. colder cells: in the viable embryos the warmer cell division rate slowed down related to its expected rate by a larger factor than that of the cooler cell, hence restoring what would have otherwise been an out-of-sequence division pattern. Thus, it appears that the embryos that respond most dramatically and correct the

510 discordance most effectively are the most likely to survive. We propose that this effect
511 may reflect an active process that corrects for noise-induced drift and ensures a faithful
512 output.

513 Our data also support the existence of a later-acting compensatory system that
514 correct errors after the early cell divisions. Although some "P_1-warm" embryos failed to
515 correct for the discordant conditions and reversed the stereotyped division sequence,
516 they could nonetheless proceed through apparently relatively normal development,
517 resulting in a worm-like, albeit lethal, animal (Fig. 6). Rapid signaling events in the early
518 embryo depend on precise geometry of cells (for example, in the induction of both gut in
519 the EMS lineage and of ABp-specific fate by the P_2 cell; [22,58–64]). Our observations
520 suggest that morphogenesis can be coordinated and corrections made even after an
521 embryo with aberrant cellular arrangements has formed. This finding is consistent with
522 reports that, at elevated T's, much later mid-stage embryos show variability in cell
523 positions and cell lineage patterns and yet resolve into normal healthy animals through
524 normal cell repositioning and morphogenesis [21,65,66].

525

526 **Potential regulatory processes in compensation to discordance**

527 It will be of interest to understand the molecular machinery that might mediate the
528 profound cell division timing adjustments we have observed in embryos exposed to the T
529 gradient. The asynchrony of AB and P_1 division timing is known to reflect at least two
530 checkpoint-based regulatory systems. First, cell-size-dependent control by ATL-1 and
531 CHK-1 accounts for approximately 40% of the difference in cell cycle timing between AB
532 and P_1 [29]. The other system acts independently of cell size and depends on localization

of PLK-1 and CDC-25.1 in P_1 [67,68]. The tight regulation of the cell cycle seen in early in *C. elegans* embryogenesis is also apparent in mice, in which DNA damage and spindle assembly checkpoints are active [69,70]; however, this does not appear to be the case in other vertebrates, including Xenopus and zebrafish [71,72], in which these cell division regulatory systems are enabled only after the midblastula transition. It is conceivable that regulatory events that influence either the ATL-1/CHK-1 checkpoint system or the PLK-1 checkpoint system in the early *C. elegans* embryo could mediate the response to discordant conditions of the T gradient.

A prominent example of a system that coordinates cellular timing during development, thereby ensuring highly reproducible pattering, is the segmentation clock for somitogenesis in vertebrate embryos, which is controlled in part by Notch signaling [17–19,73]. Notch signaling is also used to specify cell identities throughout development in *C. elegans*, including in the very early embryo [22,74]. It is intriguing to note that the maternally provided GLP-1 Notch receptor is differentially expressed as early as the two-cell stage in *C. elegans*, where it is translated in AB but not P_1. Moreover, LIN-12, the other Notch receptor, is zygotically expressed as early as the 24-cell stage [75] and its (presumably maternal) transcript has been detected at low levels as early as the one-cell stage [76,77]. While it is tempting to speculate that Notch signaling might function in coordination of AB and P_1 division, no Notch ligand has been found to be expressed as early as the two-cell stage, though the APX-1 ligand is expressed, and functions, in its daughter P_2; [63]. It will be of interest to test whether early embryos lacking both Notch receptors show an altered response to a T gradient, in which case Notch signaling might

555 be implicated in mediating communication between AB and P_1 that coordinates their
556 division timing.
557
558 **Other potential implications of compensation to a T gradient**
559 Our findings may be relevant to understanding the factors the dictate the T limits
560 over which poikilotherms are able to develop successfully. It is generally accepted that
561 these limits reflect, in part, the T range over which critical intracellular components are
562 able to function properly. Studies of closely related species of nematodes and flies
563 demonstrate that there is a uniform scaling of development in time as a function of T
564 [51,78]. The exponential nature of the T-dependent rates of events in the one-cell *C.*
565 *elegans* embryo [51], and the T-dependent model of the first cell divisions described here,
566 raise the possibility that the failure of development at T's that are just outside the range
567 for successful development might also be the result of divergence of cell division clocks
568 within the developing animal as a result of a breakdown in the compensation system.
569 Finally, the apparent compensatory system suggested by these findings may
570 account for observations that human embryos are particularly susceptible to failure early
571 during embryogenesis, which appears to be coupled with mismatches in cellular timing in
572 very early embryonic cells [79]. An early-acting system that detects and compensates for
573 cell-cycle timing defects might function as a global developmental abort system in higher
574 organisms, particularly when full-term development is costly.
575

Materials and Methods

Construction of a microfluidic device to generate a stable steep T gradient.

The microfluidic device consists of two main layers: a backplane, containing the vias and electrodes of the device and a second layer of microchannels placed on top of the backplane (see supplemental text for detailed method). The device uses a platinum Joule micro-heater to establish the high T side of the gradient. The Joule heater along with four micro resistive thermal devices (RTDs) acting as local T sensors, are simultaneously patterned through micro-lithography and metal deposition on a glass substrate. Electrical current generates an approximate cylindrical dispersal of heat around and away from the Joule heater. To reject the heat and focus the T gradient, a chilled fluid mixture is flowed underneath and in contact with the glass substrate on the surface opposite from that containing the heater. The magnitude of the T gradient as well as its rate of change is controlled by varying the T of the fluid underneath the glass, as well as the power through the Joule heater. A microfluidic channel with “trapping pillars” to capture and orient *a C. elegans* embryo within the T gradient, is placed on top of the heater. The microfluidic channel terminates at the end of the glass substrate where microbore tubing is affixed in a manner that allows embryos to be introduced into the device.

Characterization of the in-device T gradient

The T gradients generated in the microfluidic device were characterized using thermometric microscopy to correlate the fluorescence intensity of Rhodamine B with T and measurements from on board resistive thermal sensors or devices (RTDs). After

599 ensuring that there are no bubbles in the microchannels, the water was replaced by a
600 dilute solution of dextran conjugated Rhodamine B (DCRB). To construct a standard
601 curve relating T at each point in the channels with fluorescence intensity, approximately
602 30-60 fluorescence images of the DCRB filled microchannels are taken at each T
603 between 30°C and 1.5°C which is achieved by regulating the voltage applied to the Joule
604 heater. The T at each point in the device is estimated by the classical least squares model
605 for each pixel. 2D Finite element analysis was performed using Comsol Multiphysics
606 versions 5.1-5.2a. Built-in material properties were used, with the notable exceptions of
607 the physical parameters for SU-8, and NOA 81, which were both estimated to have the
608 physical properties of polyethylene. Cooling fluid flow under the device was assumed to
609 be laminar. The resistance measured by the different RTDs in the gradient was correlated
610 with the T using standard least squares fitting (see supplemental text).
611
612 **Embryo preparation and loading**
613 Embryo experiments were conducted with the *C. elegans* laboratory reference
614 strain N2 which was maintained as described by Stiernagle [80]. Strains were maintained
615 at either room T (18-22°C) or in a 15°C incubator. Young adult worms are cut open under
616 a dissecting scope in osmotically balanced Edgars egg salts solution as described by
617 Edgar and McGhee [59] and selected embryos are transferred via mouth pipette to the
618 end of tubing that is connected to the inlet ports of the microfluidic device. One-cell
619 embryos were loaded into the device either before pronuclear meeting or immediately
620 after. For two-cell embryos, we continued to track development outside of the microfluidic
621 device until the first membrane cleavage, at which point they were loaded into the device,

using a syringe pump. Embryos generally reached the capture region of the device within 30-60 seconds. A flow of 500nl/min was maintained in the device while embryos were in the device to ensure that they did not experience hypoxic conditions. Embryos were unloaded from the device by operating the syringe in reverse. The embryos were then transferred with a mouth pipette to a standard agar plate seeded with E. coli OP50 and incubated at room T and scored if they hatched or were dead ~ 24 hours later. Embryos with reversed sequence of cell division were observed 24 hours later on a Nikon Eclipse Ti at 100X magnification

Estimation of cell division rate

Embryos were imaged on an upright Nikon Microphot microscope at 10 second intervals. Cell division interval was determined as time between successive cytokinesis as inferred by the first image that shows apparent completion of membrane pinching. For embryos loaded after the first division, the rate of division was estimated using the measured room T and the linear model of time of division as a function of T.

Acknowledgements

Nematode strains used in this work were provided by the Caenorhabditis Genetics Center, which is funded by the National Institutes of Health - Office of Research Infrastructure Programs (P40 OD010440). This work was supported by grants from NIH (#1 R21 HD075292).

Figure legends

Figure 1. Microfluidic device design. A) The two-cell *C. elegans* embryo is subjected to a T gradient. Normally, in absence of a gradient under constant uniform Ts, AB divides before P_1. In a gradient AB and P_1 divide with rates of division determined by the T experienced by the respective cell. In absence of a coordination mechanism between the two cells (left), it is possible to establish a T differential at which the order of division of AB and P_1 is reversed wherein the warmer P_1 cell divides before the cooler AB cell. If there were a coordination mechanism (right) that corrects for the discordant conditions, the embryo should resist the T-dependent rates of division allowing for the canonical order of AB and P_1 divisions. B) Microfluidic device used to capture and orient embryo in a T gradient. In the example shown here the embryo is oriented such that the posterior smaller P_1 blastomere is closer to the heating element and experiences a warmer T while the larger anterior AB blastomere experiences a cooler T. C-F) Schematic of the layout of device at four scales. C) Macro view of the device. Blue indicates channels, orange indicates T sensors (RTD) and magenta indicates a Joule heater. D) Closer view of T sensing regions of RTDs and capture region. E) View showing all three channels, capture regions for embryos in each channel, Joule heater, and RTDs close to Joule heater. F) Closeup of a single capture region and example of embryo size and placement. Spacing between heater and lower RTDs is 10µm. Width of the heater and RTDs is 10µm

Figure 2. Characterization of the T gradient in the microfluidic device. Characterization and modeling of the T gradient in the microfluidic device using Dextran

667 conjugated Rhodamine B (DCRB). A) Yellow circle represents the pixel intensities of
668 DCRB analyzed. B) (Left) Linear model relating fluorescence intensity of DCRB to T and
669 (right) 97.5% confidence interval distance from model for the inverse linear model of
670 intensity to T, as function of T. C) False coloring heat map of T distribution in device during
671 operation. D) Black data points and error bars indicate the average Ts and standard error
672 across all three channels as a function of position in the channel. X=0 indicates the center
673 of the Joule heating element. Blue line is the model estimate of Ts along the interior
674 bottom of the microfluidic device. Black line is the model estimate of the depth average T
675 in the channel and Orange line is the model estimate of T in the embryo. Blue dots
676 correspond to RTD T measurements at the position relative to the heater
677
678 **Figure 3. Survival in the T gradient is dependent on both the magnitude of the**
679 **gradient and orientation of the embryo.** A) Fraction of embryos completing
680 development in the microfluidic channel. B) Survival of mixed stage early embryos (1- 4
681 cells) after ~ 1 hour in the device and then unloaded and placed on agar plates to
682 complete development. C) Survival of embryos in gradients of different magnitudes.
683 Pooled data for embryos in both orientations, embryos with anterior (AB) warm, and
684 embryos with posterior (P_1) warm in T gradients of different magnitudes are shown. The
685 rightmost graph represents embryos loaded prior to first cell division in a 5°C T gradient
686 (Fisher exact test $p<0.05$ **$p<0.01$ ***$p<0.001$)
687
688 **Figure 4. Cell division rates of individual blastomeres in the T gradient.** Linear model
689 of division time of AB (A) and P_1 (B) as a function of T. Notched box plots are data at

690 various Ts. Innermost line indicates linear model. Next outer pair of lines indicate 95%
691 confidence interval while the outermost pair of lines indicate 95% prediction interval. C-
692 H) Notched box plot of division time for AB (left) and P_1 (right) at the corresponding T
693 plotted over the corresponding model. In both AB and P_1 plots, the left box corresponds
694 to when the cell is close to the heater and the right box corresponds to when the cell is
695 away from the heater. This cohort of embryos were loaded after formation of first
696 cleavage. I and J) same as C-H except these embryos were loaded in a 5°C gradient
697 before the first cleavage.
698
699 **Figure 5. Analysis of deviations in division rates of AB and P_1.** A) Explanatory graph
700 for fold change in division time for whole embryo. B) Scatter plot for whole embryo
701 behavior when (left) P_1 is warm and (right) AB is warm. Black data points represent
702 embryos that did not survive to hatching while blue and red represent those that did.
703 Crosses and error bars are mean and SE. C) Mean, SE, and 95% CI for fold changes in
704 AB and P_1, based on orientation and survival. Blue-embryos with P_1 warmer than AB,
705 Red-embryos with AB warmer than P_1. Black standard error bars identify populations that
706 did not survive. Colored ellipses represent two-dimensional 95%CI for each population.
707 The black data point at origin and the surrounding gray ellipse are the mean and 95%CI
708 respectively of control embryos at a uniform T.
709
710 **Figure 6. Relatively normal morphogenesis following out of sequence divisions of**
711 **AB and P_1.** Time lapse images and outline of early cell divisions of AB and P_1. Top panel:
712 stereotyped control embryos with the larger anterior AB cell dividing before the smaller

713 posterior cell P_1 at a uniform permissive T. Bottom and middle panels: example of two
714 embryos experiencing a reversal of the division sequence of AB and P_1, along with 100X
715 DIC image of an arrested embryo~ 24 hours after being in T gradient. The embryo had
716 progressed through morphogenesis and elongation despite the reversed sequence of AB-
717 P_1 divisions.
718

719 **Figure 1. Microfluidic device design**

720

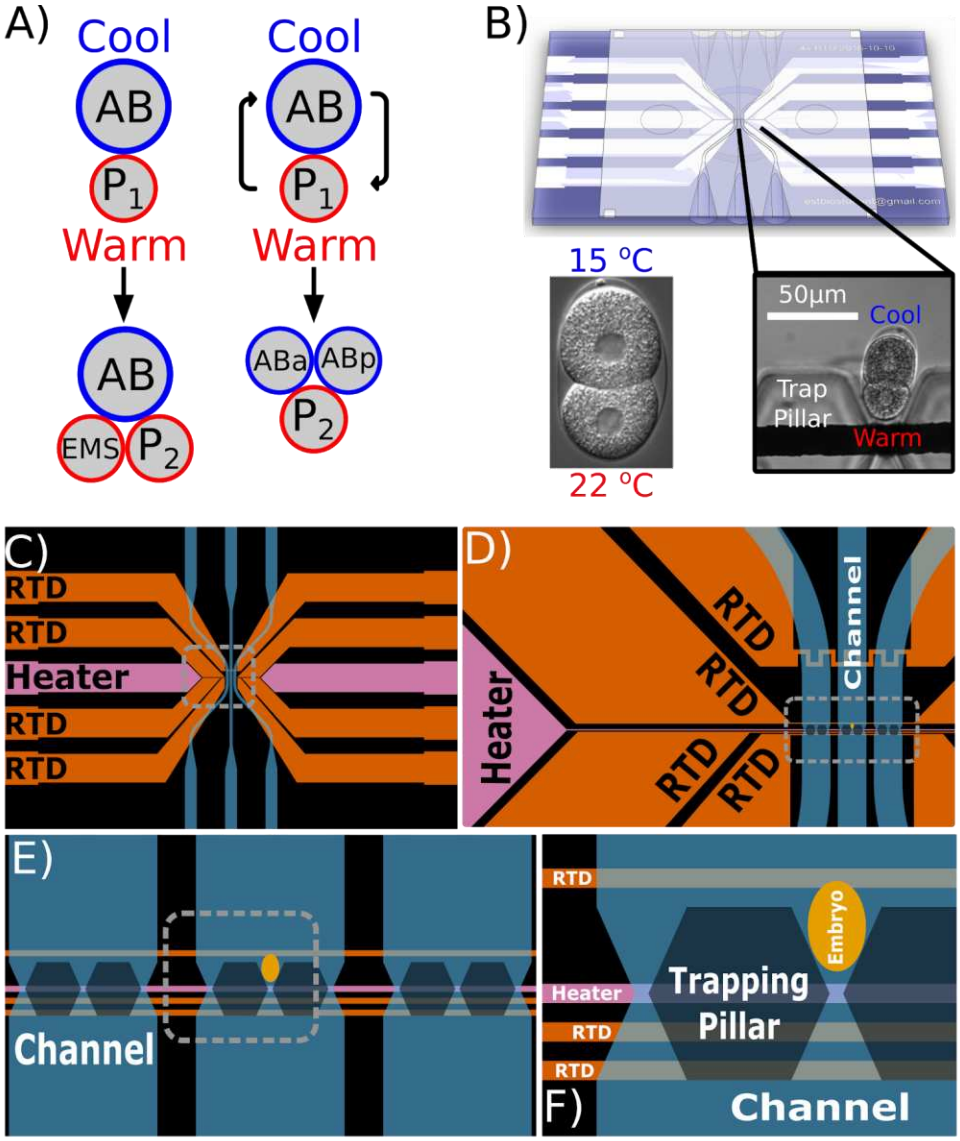

721 **Figure 2. Characterization of the T gradient in the microfluidic device.**

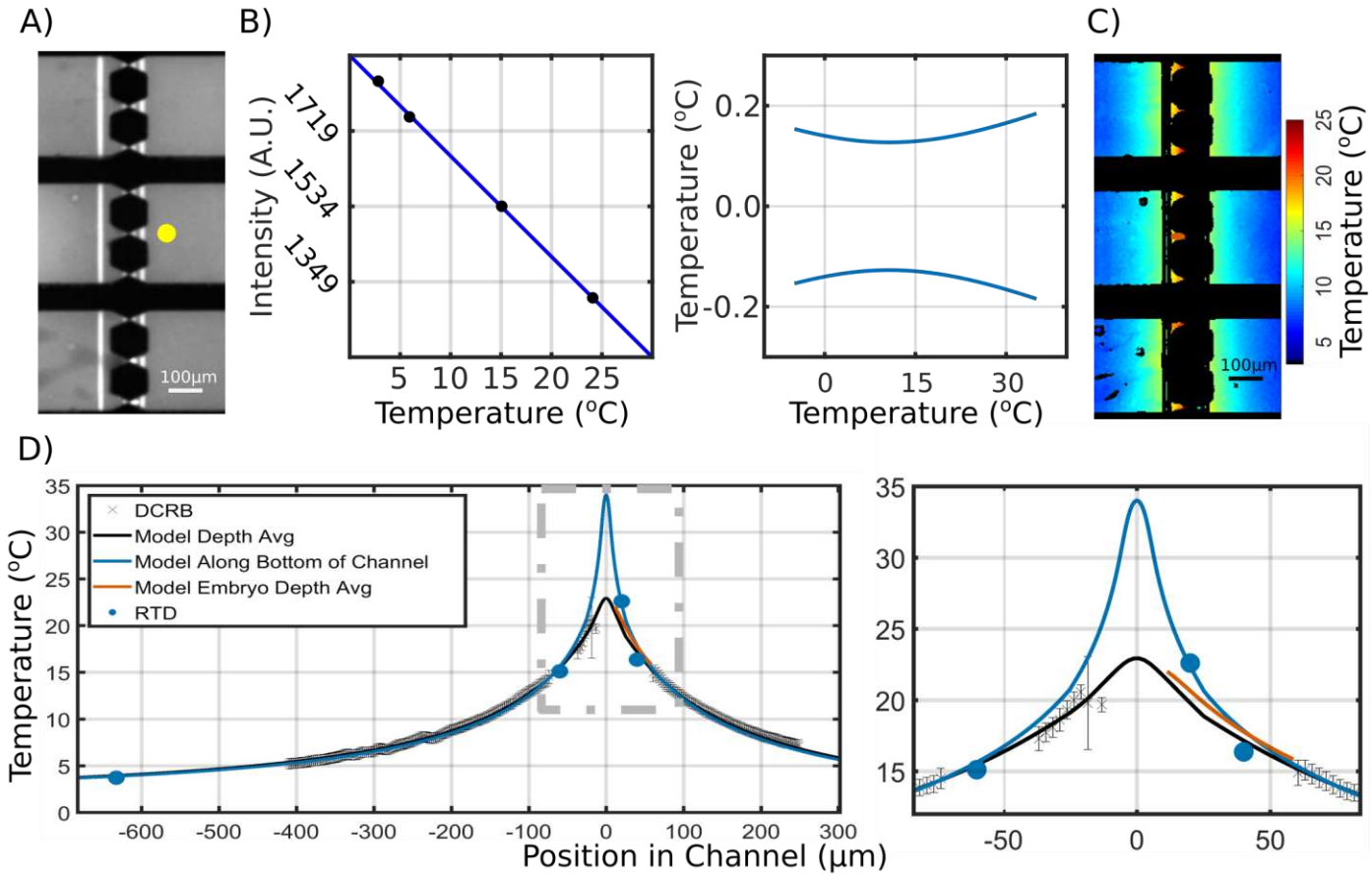

722

723 **Figure 3. Survival in the T gradient is dependent on both the magnitude of the**

724 **gradient and orientation of the embryo**

725

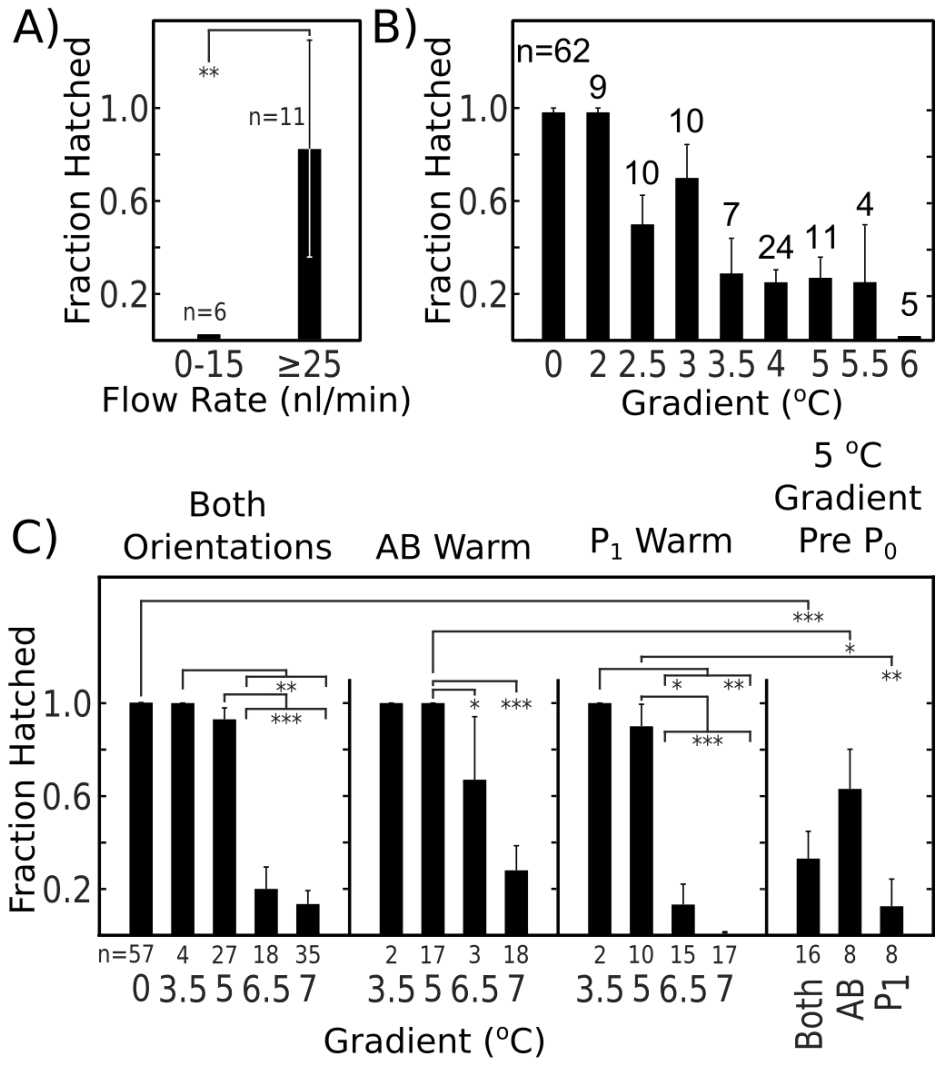

726

727

728 **Figure 4. Cell division rates of individual blastomeres in the T gradient**

729

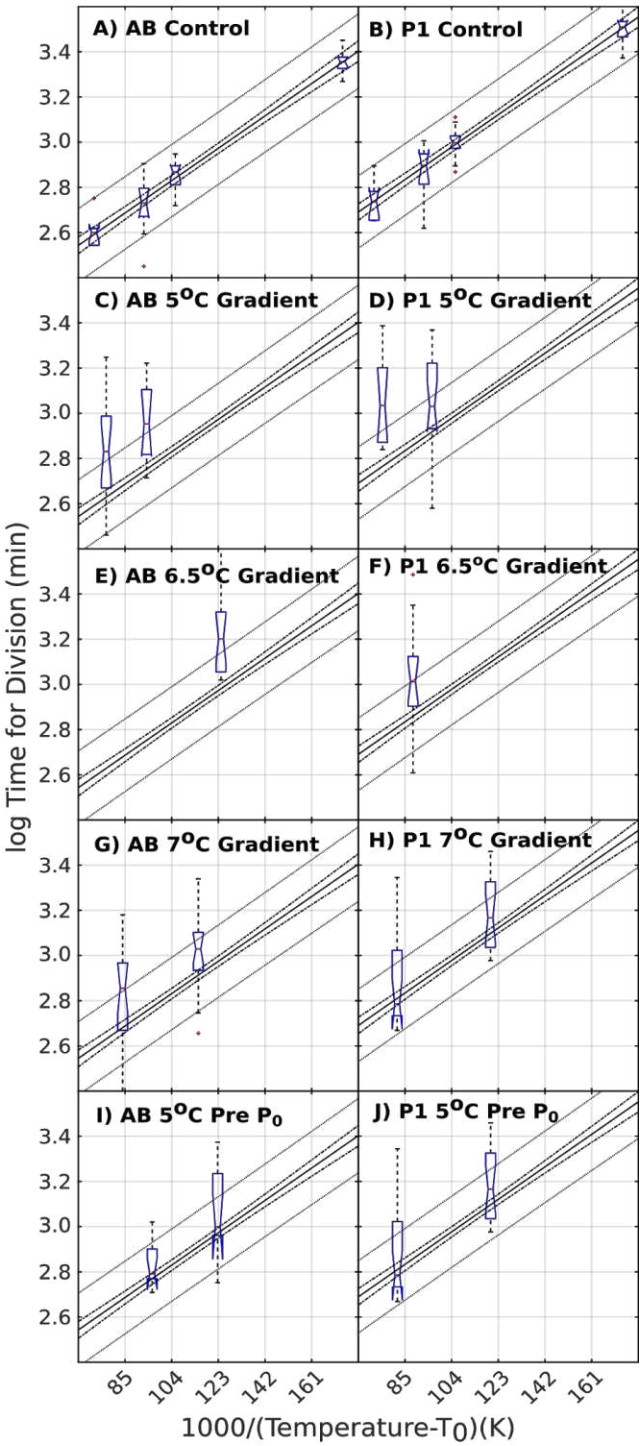

730

731 **Figure 5. Analysis of deviations in division rates of AB and P_1.**

732

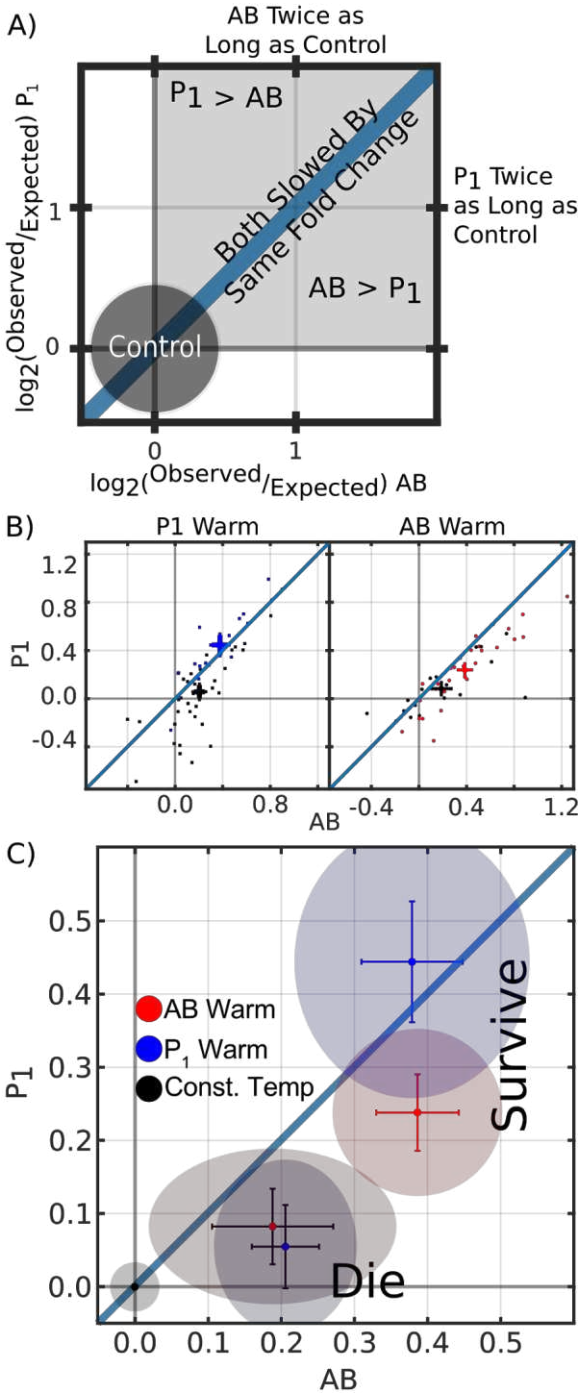

733 **Figure 6. Relatively normal morphogenesis following out of sequence divisions of**
734 **AB and P_1.**

735

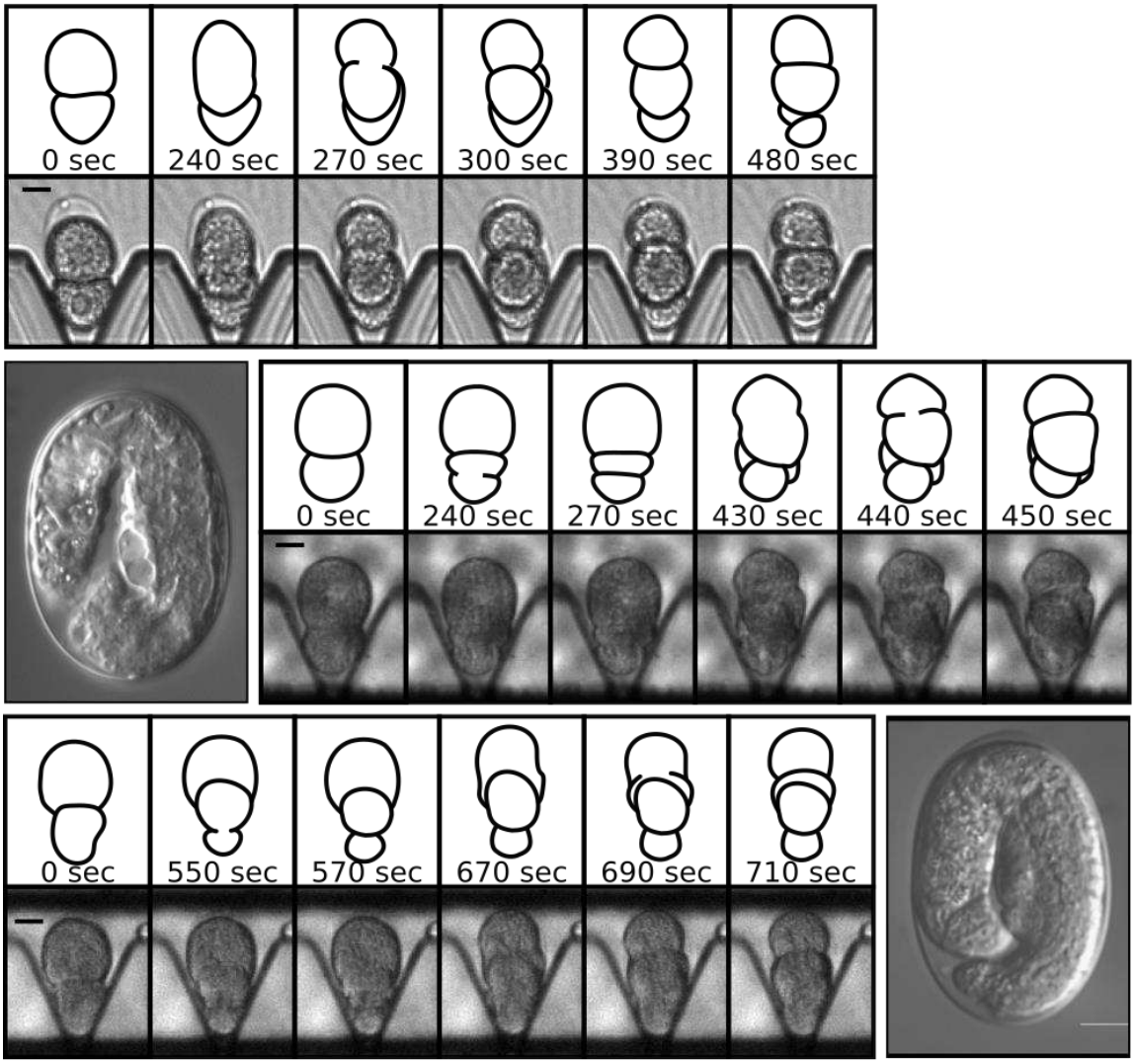

1. Felix MA, Wagner A. Robustness and evolution: concepts, insights and challenges from a developmental model system. Hered. 2008;100: 132–140. doi:10.1038/sj.hdy.6800915
2. Mantikou E, Wong KM, Repping S, Mastenbroek S. Molecular origin of mitotic aneuploidies in preimplantation embryos. Biochimica et Biophysica Acta - Molecular Basis of Disease. Elsevier; 2012. pp. 1921–1930. doi:10.1016/j.bbadis.2012.06.013
3. Houchmandzadeh B, Wieschaus E, Leibler S. Establishment of developmental precision and proportions in the early Drosophila embryo. Nature. 2002;415: 798–802. doi:10.1038/415798a
4. Barbash-Hazan S, Frumkin T, Malcov M, Yaron Y, Cohen T, Azem F, et al. Preimplantation aneuploid embryos undergo self-correction in correlation with their developmental potential. Fertil Steril. 2009;92: 890–896. doi:10.1016/j.fertnstert.2008.07.1761
5. Kosubek A, Klein-Hitpass L, Rademacher K, Horsthemke B, Ryffel GU. Aging of Xenopus tropicalis Eggs Leads to Deadenylation of a Specific Set of Maternal mRNAs and Loss of Developmental Potential. Veenstra GJC, editor. PLoS One. 2010;5: e13532. doi:10.1371/journal.pone.0013532
6. Wood WB, Hecht R, Carr S, Vanderslice R, Wolf N, Hirsh D. Parental effects and phenotypic characterization of mutations that affect early development in Caenorhabditis elegans. Dev Biol. 1980;74: 446–469.
7. Ward S, Miwa J. Characterization of temperature-sensitive, fertilization-defective mutants of the nematode caenorhabditis elegans. Genetics. 1978;88: 285–303.
8. Ben-David E, Burga A, Kruglyak L. A maternal-effect selfish genetic element in Caenorhabditis elegans. Science (80-). 2017;356: 1051–1055. doi:10.1126/SCIENCE.AAN0621
9. Yeyati PL, van Heyningen V. Incapacitating the evolutionary capacitor: Hsp90 modulation of disease. Curr Opin Genet Dev. 2008;18: 264–272. doi:10.1016/j.gde.2008.07.004
10. Rutherford S, Hirate Y, Swalla BJ. The Hsp90 capacitor, developmental remodeling, and evolution: the robustness of gene networks and the curious evolvability of metamorphosis. Crit Rev Biochem Mol Biol. 2007;42: 355–372. doi:10.1080/10409230701597782
11. Rutherford SL, Lindquist S. Hsp90 as a capacitor for morphological evolution. Nature. 1998;396: 336–342. doi:10.1038/24550
12. Rohner N, Jarosz DF, Kowalko JE, Yoshizawa M, Jeffery WR, Borowsky RL, et al. Cryptic variation in morphological evolution: HSP90 as a capacitor for loss of eyes in cavefish. Science (80-). 2013;342: 1372–1375. doi:10.1126/science.1240276
13. Sollars V, Lu X, Xiao L, Wang X, Garfinkel MD, Ruden DM. Evidence for an epigenetic mechanism by which Hsp90 acts as a capacitor for morphological evolution. Nat Genet. 2003;33: 70–74. doi:10.1038/ng1067
14. Queitsch C, Sangster TA, Lindquist S. Hsp90 as a capacitor of phenotypic variation. Nature. 2002;417: 618–624. doi:10.1038/nature749
15. Eldar A, Shilo BZ, Barkai N. Elucidating mechanisms underlying robustness of morphogen gradients. Current Opinion in Genetics and Development. Elsevier Current Trends; 2004. pp. 435–439. doi:10.1016/j.gde.2004.06.009
16. Cheung D, Miles C, Kreitman M, Ma J. Adaptation of the length scale and amplitude of the

780 Bicoid gradient profile to achieve robust patterning in abnormally large Drosophila
781 melanogaster embryos. Dev. 2014;141: 124–135. doi:10.1242/dev.098640
782 17. Jiang YJ, Aerne BL, Smithers L, Haddon C, Ish-Horowicz D, Lewis J. Notch signalling and the
783 synchronization of the somite segmentation clock. Nature. 2000;408: 475–479.
784 doi:10.1038/35044091
785 18. Soza-Ried C, Öztürk E, Ish-Horowicz D, Lewis J. Pulses of Notch activation synchronise
786 oscillating somite cells and entrain the zebrafish segmentation clock. Dev. 2014;141:
787 1780–1788. doi:10.1242/dev.102111
788 19. Oates AC, Morelli LG, Ares S. Patterning embryos with oscillations: Structure, function and
789 dynamics of the vertebrate segmentation clock. Development. Oxford University Press for
790 The Company of Biologists Limited; 2012. pp. 625–639. doi:10.1242/dev.063735
791 20. Sulston JE White JG Thomson JN SE, Sulston JE, Schierenberg E, White JG, Thomson JN. The
792 embryonic cell lineage of the nematode Caenorhabditis elegans. Developmental Biology
793 1983 pp. 64–119. doi:10.1016/0012-1606(83)90201-4
794 21. Bao Z, Zhao Z, Boyle TJ, Murray JI, Waterston RH. Control of cell cycle timing during C.
795 elegans embryogenesis. Dev Biol. 2008/04/24. 2008;318: 65–72. doi:S0012-
796 1606(08)00183-8 [pii]10.1016/j.ydbio.2008.02.054
797 22. Priess JR. Notch signaling in the C. elegans embryo. WormBook. 2005; 1–16.
798 doi:10.1895/wormbook.1.4.1
799 23. Priess JR, Thomson JN. Cellular interactions in early C. elegans embryos. Cell. 1987;48:
800 241–250.
801 24. Deppe U, Schierenberg E, Cole T, Krieg C, Schmitt D, Yoder B, et al. Cell lineages of the
802 embryo of the nematode Caenorhabditis elegans. Proc Natl Acad Sci U S A. 1978;75: 376–
803 380.
804 25. Schierenberg E, Wood WB. Control of cell-cycle timing in early embryos of Caenorhabditis
805 elegans. Dev Biol. 1985;107: 337–354.
806 26. Robertson SM, Medina J, Lin R. Uncoupling Different Characteristics of the C. elegans E
807 Lineage from Differentiation of Intestinal Markers. Goldstein B, editor. PLoS One. 2014;9:
808 e106309. doi:10.1371/journal.pone.0106309
809 27. Edgar LG, Goldstein B. Culture and manipulation of embryonic cells. Methods Cell Biol.
810 107: 151.
811 28. Goldstein B. Induction of gut in Caenorhabditis elegans embryos. Nature. 1992;357: 255–
812 257.
813 29. Brauchle M, Baumer K, Gönczy P. Differential activation of the DNA replication checkpoint
814 contributes to asynchrony of cell division in C. elegans embryos. Curr Biol. 2003;13: 819–
815 827. doi:10.1016/S
816 30. Arata Y, Takagi H, Sako Y, Sawa H. Power law relationship between cell cycle duration and
817 cell volume in the early embryonic development of Caenorhabditis elegans. Front Physiol.
818 2015;5: 529. doi:10.3389/fphys.2014.00529
819 31. Sawa H. Control of cell polarity and asymmetric division in C. elegans. Curr Top Dev Biol.
820 2012/11/13. 2012;101: 55–76. doi:10.1016/b978-0-12-394592-1.00003-x
821 32. Rose L, Gonczy P. Polarity establishment, asymmetric division and segregation of fate
822 determinants in early C. elegans embryos. WormBook. 2014; 1–43.
823 doi:10.1895/wormbook.1.30.2

33. Gonczy P, Rose LS. Asymmetric cell division and axis formation in the embryo. WormBook. 2005; 1–20. doi:10.1895/wormbook.1.30.1
34. Francklyn CS. DNA polymerases and aminoacyl-tRNA synthetases: shared mechanisms for ensuring the fidelity of gene expression. Biochemistry. 2008;47: 11695–11703. doi:10.1021/bi801500z
35. Ganai RA, Johansson E. DNA Replication-A Matter of Fidelity. Mol Cell. 2016/06/04. 2016;62: 745–755. doi:10.1016/j.molcel.2016.05.003
36. Wang Y, Badea T, Nathans J. Order from disorder: Self-organization in mammalian hair patterning. Proc Natl Acad Sci U S A. 2006;103: 19800–19805. doi:10.1073/pnas.0609712104
37. Briscoe J, Small S. Morphogen rules: Design principles of gradient-mediated embryo patterning. Development (Cambridge). Company of Biologists Ltd; 2015. pp. 3996–4009. doi:10.1242/dev.129452
38. Schweisguth F, Corson F. Self-Organization in Pattern Formation. Developmental Cell. Cell Press; 2019. pp. 659–677. doi:10.1016/j.devcel.2019.05.019
39. Martinez Arias A, Steventon B. On the nature and function of organizers. Development (Cambridge). Company of Biologists Ltd; 2018. doi:10.1242/dev.159525
40. Tautz D. Redundancies, development and the flow of information. BioEssays. 1992;14: 263–266. doi:10.1002/bies.950140410
41. Zhang Z, Zwick S, Loew E, Grimley JS, Ramanathan S. Mouse embryo geometry drives formation of robust signaling gradients through receptor localization. Nat Commun. 2019;10: 1–14. doi:10.1038/s41467-019-12533-7
42. Akieda Y, Ogamino S, Furuie H, Ishitani S, Akiyoshi R, Nogami J, et al. Cell competition corrects noisy Wnt morphogen gradients to achieve robust patterning in the zebrafish embryo. Nat Commun. 2019;10: 1–17. doi:10.1038/s41467-019-12609-4
43. Averbukh I, Lai SL, Doe CQ, Barkai N. A repressor-decay timer for robust temporal patterning in embryonic drosophila neuroblast lineages. Elife. 2018;7. doi:10.7554/eLife.38631
44. Niemuth J, Wolf R. Developmental asynchrony caused by steep temperature gradients does not impair pattern formation in the wasp, Pimpla turionellae L. Roux Arch Dev Biol. 1995/08/01. 1995;204: 444–452. doi:10.1007/bf00360852
45. Lucchetta EM, Lee JH, Fu LA, Patel NH, Ismagilov RF. Dynamics of Drosophila embryonic patterning network perturbed in space and time using microfluidics. Nature. 2005/04/29. 2005;434: 1134–1138. doi:10.1038/nature03509
46. Richards JL, Zacharias AL, Walton T, Burdick JT, Murray JI. A quantitative model of normal Caenorhabditis elegans embryogenesis and its disruption after stress. Dev Biol. 2013;374: 12–23. doi:10.1016/j.ydbio.2012.11.034
47. Zacharias AL, Murray JI. Combinatorial decoding of the invariant C. elegans embryonic lineage in space and time. Genesis. 2016;54: 182–197. doi:10.1002/dvg.22928
48. Byerly L, Cassada RC, Russell RL. The life cycle of the nematode Caenorhabditis elegans. I. Wild-type growth and reproduction. Dev Biol. 1976;51: 23–33. doi:10.1016/0012-1606(76)90119-6
49. Folkmann AW, Seydoux G. Spatial regulation of the polarity kinase PAR-1 by parallel inhibitory mechanisms. 2019; doi:10.1242/dev.171116

50. Singh D, Pohl C. Coupling of rotational cortical flow, asymmetric midbody positioning, and spindle rotation mediates dorsoventral axis formation in C. elegans. Dev Cell. 2014;28: 253–267. doi:10.1016/j.devcel.2014.01.002
51. Elegans C, Briggsae Graphical C, Begasse ML, Grill SW, Hyman AA, Leaver M, et al. Temperature Dependence of Cell Division Timing Accounts for a Shift in the Thermal Limits of Temperature Dependence of Cell Division Timing Accounts for a Shift in the Thermal Limits of C. elegans and C. briggsae. Cell Rep. 2015;10: 647–653. doi:10.1016/j.celrep.2015.01.006
52. Nakamura K, Takayanagi T, Sato S. A modified arrhenius equation. Chem Phys Lett. 1989;160: 295–298. doi:10.1016/0009-2614(89)87599-2
53. Motoyama N, Naka K. DNA damage tumor suppressor genes and genomic instability. Curr Opin Genet Dev. 2004;14: 11–16. Available: http://www.ncbi.nlm.nih.gov/entrez/query.fcgi?cmd=Retrieve&db=PubMed&dopt=Citation&list_uids=15108799
54. O'Neil N, Rose A. DNA repair. WormBook. 2006; 1–12. doi:10.1895/wormbook.1.54.1
55. Kastan MB, Bartek J. Cell-cycle checkpoints and cancer. Nature. 2004;432: 316–323. Available: http://www.ncbi.nlm.nih.gov/entrez/query.fcgi?cmd=Retrieve&db=PubMed&dopt=Citation&list_uids=15549093
56. Gendreau S, Moskowitz IPG, Terns RM, Rothman JH. The Potential to Differentiate Epidermis is Unequally Distributed in the AB Lineage. Dev Biol. 1994; doi:10.1006/dbio.1994.1355
57. Djabrayan NJ, Dudley NR, Sommermann EM, Rothman JH. Essential role for Notch signaling in restricting developmental plasticity. Genes Dev. 2012/11/06. 2012;26: 2386–2391. doi:10.1101/gad.199588.112
58. Boyle MJ, Seaver EC. Developmental expression of foxA and gata genes during gut formation in the polychaete annelid, Capitella sp. I. Evol Dev. 2008;10: 89–105. doi:10.1111/j.1525-142X.2007.00216.x
59. Edgar LG, McGhee JD. Embryonic expression of a gut-specific esterase in Caenorhabditis elegans. Dev Biol. 1986;114: 109–118.
60. Maduro MF. Gut development in C. elegans. Semin Cell Dev Biol. 2017;66: 3–11. doi:https://doi.org/10.1016/j.semcdb.2017.01.001
61. Moskowitz IP, Gendreau SB, Rothman JH, Ivan P. G. Moskowitz, Steven B. Gendreau, Joel H. Rothman. Combinatorial specification of blastomere identity by glp-1-dependent cellular interactions in the nematode Caenorhabditis elegans. Development. 1994;120: 3325–3338. Available: http://dev.biologists.org/content/develop/120/11/3325.full.pdf
62. Tax FE, Thomas JH. Cell-cell interactions. Receiving signals in the nematode embryo. Curr Biol. 1994;4: 914–916.
63. Mello CC, Draper BW, Priess JR. The maternal genes apx-1 and glp-1 and establishment of dorsal-ventral polarity in the early C. elegans embryo. Cell. 1994;77: 95–106.
64. Sawa H, Korswagen HC. Wnt signaling in C. elegans. WormBook. 2013; 1–30. doi:10.1895/wormbook.1.7.2
65. Bao Z, Murray JI, Boyle T, Ooi SL, Sandel MJ, Waterston RH. Automated cell lineage tracing in Caenorhabditis elegans. Proc Natl Acad Sci U S A. 2006/02/16. 2006;103: 2707–2712.

912 doi:0511111103 [pii]10.1073/pnas.0511111103
913 66. Schnabel R, Hutter H, Moerman D, Schnabel H. Assessing normal embryogenesis in
914 Caenorhabditis elegans using a 4D microscope: variability of development and regional
915 specification. Dev Biol. 1997;184: 234–265. doi:10.1006/dbio.1997.8509
916 67. Budirahardja Y, Gonczy P. PLK-1 asymmetry contributes to asynchronous cell division of C.
917 elegans embryos. Development. 2008;135: 1303–1313. doi:10.1242/dev.019075
918 68. Rivers DM, Moreno S, Abraham M, Ahringer J. PAR proteins direct asymmetry of the cell
919 cycle regulators Polo-like kinase and Cdc25. J Cell Biol. 2008;180: 877–885.
920 doi:10.1083/jcb.200710018
921 69. Wei Y, Multi S, Yang C-R, Ma J, Zhang Q-H, Wang Z-B, et al. Spindle Assembly Checkpoint
922 Regulates Mitotic Cell Cycle Progression during Preimplantation Embryo Development.
923 Wang H, editor. PLoS One. 2011;6: e21557. doi:10.1371/journal.pone.0021557
924 70. Artus J, Cohen-Tannoudji M. Cell cycle regulation during early mouse embryogenesis. Mol
925 Cell Endocrinol. 2008;282: 78–86. doi:10.1016/j.mce.2007.11.008
926 71. Clute P, Masui Y. Microtubule Dependence of Chromosome Cycles inXenopus
927 laevisBlastomeres under the Influence of a DNA Synthesis Inhibitor, Aphidicolin. Dev Biol.
928 1997;185: 1–13. doi:10.1006/dbio.1997.8540
929 72. Ikegami R, Rivera-Bennetts AK, Brooker DL, Yager TD. Effect of inhibitors of DNA replication
930 on early zebrafish embryos: evidence for coordinate activation of multiple intrinsic cell-
931 cycle checkpoints at the mid-blastula transition. Zygote. 1997;5: 153–175. Available:
932 http://www.ncbi.nlm.nih.gov/pubmed/9276512
933 73. Pourquié O. Vertebrate Somitogenesis. Annu Rev Cell Dev Biol. 2001;17: 311–350.
934 doi:10.1146/annurev.cellbio.17.1.311
935 74. Greenwald I. LIN-12/Notch signaling in C. elegans. WormBook. 2005; 1–16.
936 doi:10.1895/wormbook.1.10.1
937 75. Moskowitz IP, Rothman JH. lin-12 and glp-1 are required zygotically for early embryonic
938 cellular interactions and are regulated by maternal GLP-1 signaling in C. elegans.
939 Development. 1996;122: 4105–4117.
940 76. Hashimshony T, Feder M, Levin M, Hall BK, Yanai I. Spatiotemporal transcriptomics reveals
941 the evolutionary history of the endoderm germ layer. Nature. 2015;519: 219–222.
942 doi:10.1038/nature13996
943 77. Levin M, Hashimshony T, Wagner F, Yanai I. Developmental milestones punctuate gene
944 expression in the Caenorhabditis embryo. Dev Cell. 2012/05/09. 2012;22: 1101–1108.
945 doi:S1534-5807(12)00142-6 [pii]10.1016/j.devcel.2012.04.004 [doi]
946 78. Kuntz SG, Eisen MB, Lerat E, Vieira C, Carareto C. Drosophila Embryogenesis Scales
947 Uniformly across Temperature in Developmentally Diverse Species. Desplan C, editor. PLoS
948 Genet. 2014;10: e1004293. doi:10.1371/journal.pgen.1004293
949 79. Cruz M, Garrido N, Herrero J, Pérez-Cano I, Muñoz M, Meseguer M. Timing of cell division
950 in human cleavage-stage embryos is linked with blastocyst formation and quality. Reprod
951 Biomed Online. 2012;25: 371–381. doi:10.1016/j.rbmo.2012.06.017
952 80. Stiernagle T, Stiernagle T. Maintenance of C. elegans [Internet]. 2006 pp. 1–11.
953 doi:10.1895/wormbook.1.101.1
954

Supplementary Text

Device construction

The microfluidic device is constructed as two main layers: the backplane, containing the vias and electrodes of the device and a second layer of microchannels placed on top of the backplane. Three input and output tapering hemi-conical vias, approximately 2 mm wide, and 800-900 μm deep at the edge, are made in a 1”x3” commercially available microscope slide cut in half to 1”x1.5”. To prevent impurity migration from the microscope slide, 100-150 nm of SiO2 is reactive sputter deposited on the backplane. Electrodes of 10 nm Ti followed by 100 nm of Pt were patterned on microscope slides using standard negative photoresist clean room photolithography. The electrode face of the device is covered with an approximate 2 μm layer of SU-8 2002 (MicroChem Corp., Westborough, MA). Centered on the device, an ~ 1cm diameter and 750-800 μm deep circular cut, under and in the opposite face of the glass, is HF etched into the glass which allowed a steep T gradient of 7.5°C by reducing the thickness of the coverslip and ensuring the heat was dissipated away by circulation of chilled water. A positive master mold of our microfluidic channel design was dry etched 40 μm deep into a 3” silicon wafer with a negative PDMS mold made from the silicon wafer using standard soft lithography techniques [1]. The microfluidic “sticker” layer of the device is constructed consistent with methods developed by Bartolo et al. [2], and is placed on top of the electrodes with the capture pillars of the device centered on the electrodes of the backplane. 0.03" outer diameter PTFE tubing is inserted into the device vias, and secured with two-part epoxy.

Device is mounted on a custom-built device holder/flow cell that allows bulk fluid flow underneath and in contact with the outside bottom surface of the microfluidic device.

Tubing (~0.25" ID PDMS) connects the flow cell to a water circulator filled with DI water and ethylene glycol in a ratio of 4:1. Flow rate through the fluid cell is on the order of 19 ml/sec. The water circulator is used to set the background T of the device. Device holder/flow cell and device are loaded into a custom rig on an upright microscope. A custom environmental chamber enclosing the microscope is maintained at a slight positive pressure with sub 0°C dew point laboratory supplied air to prevent condensation on device during operation.

Characterization of the T gradient

Effect of T on the fluorescence response of Rhodamine B has been extensively studied and its quantum yield is highly T dependent[3–5]. It has been previously reported that a solution of dextran-conjugated fluorophores can aggregate, resulting in an apparent increase in quantum efficiency of the fluorophore, and that the aggregation rate is T dependent [6]. To address this concern, we performed our measurements with a flow of the solution running during measurements. To ensure the introduced flow would not affect the T profile of the device we calculated the expected flow rate of our device for which the Pe would equal one and found it to be on the order of 1-2µl/min. We then measured the effect of fluid flow above and below this threshold with thermometric microscopy utilizing DCRB. We found that a flow of 2µl/min did not affect the T profile of the gradient, while at flow of 15µl/min shifted the T profile in the direction of flow. In later devices, in addition to characterization of the T gradient with thermometric microscopy, we also included resistive thermal sensors or devices (RTDs) [7] in the T gradient region of the device. The device is placed in a well stirred ice bath and allowed to come up to room T while

measuring the T of the bath with thermocouples and resistance of the RTDs. Standard least squares fitting is used to relate the RTD measurements with T. We found a highly linear correlation between T and the measured resistance, and modeled the relationship between the two using a least squares linear model. R^2 values of linear models fitting resistance to Ts ranging from 0°C to 20°C were typically on the order of 0.999. To verify that the RTDs were primarily measuring the T in the region of the T gradient, and not the electrode leads leading up to that region, we measured the resistance of the patterned RTDs with the device mounted on a flow cell that flowed a fixed and measured T of water below the region of the device where the T gradient is established. We found that our T measurements were within 1°C of the experiment in which the device was fully submerged.

During normal operation of the device, the device is not submerged in fluid. To verify that our T measurement was a reasonable estimate of the T in the channel, and not just the bottom of the channel, we constructed a modified flow cell that allowed the flow of the T setting water both underneath as well as over the top of the device. We found that the average difference in T measured between when the top of the device is exposed to air, and when it is sandwiched between flowing fluid was on the order of a third of a degree.

Modeling the apparent intra-embryonic T gradient.

We modeled the embryo as a 50x30 μm spheroid with thermal conductivity equal to that of water, $k_{cytoplasm}$=0.6 W/m-K [8], and an insulating eggshell of 300 nm thickness [9]. Although cytoplasm is a gel matrix, thermal conductivity of a gel, for example a

concentrated protein solution of 10% gelatin, is only 5% lower in conductivity than water [10]. While thermal conductivity of nematode eggshells has not been measured, a model of *Drosophila* embryos [8] used $k_{shell}=k_{paraffin}$ wax =0.25 W/m-K, 10x more insulating than an avian eggshell. Using this extreme value in our simulation, the intra-embryonic gradient was reduced by only 1%. We also considered the possibility that extremely active fluid circulation within the embryo might overcome the T gradient within the embryo by convective transport. The Peclet number (Pe) of a system indicates whether convection or diffusion dominates in determining the distribution of heat. A Pe of one indicates a system where convection and diffusion are in balance. Values higher than one indicate convection dominates and values lower than one indicate diffusion dominates. The maximum known cytoplasmic streaming velocity in the *C. elegans* embryo of 7 μm/min [11], cannot overcome thermal diffusion at this scale as the Peclet (Pe) number of the embryo with known dimensions and expected possible highest velocity is only $2.5x10^{-5}$. Thus, the T gradient within the embryo is in close accordance with the external T gradient in the microfluidic device.

Verification that the microfluidic device is compatible with embryonic development

To verify compatibility of the device with embryo development, a cohort of early stage embryos (1-8 cell stage) were loaded into the device and allowed to develop to hatching while in the device. Below a certain threshold of flow, the embryos tended to arrest during development and or not complete development. This finding was consistent with the material from which the device was constructed, NOA81, being gas impermeable [12]. Flow rates in excess of 25nl/min prevented arrest of embryos during development. Having previously calculated the Pe of the device and measured the effect of fluid flow

below the critical rate, we were confident that a flow rate of 100-500nl/min within the device would not affect the T profile of the device while simultaneously creating a biologically compatible environment. Our real time RTD measurements of T in the device in our later experiments also demonstrated that the T profile at these slower flow rates remained similar to those without flow. To determine the effect of loading and unloading on the survival of the embryos, we loaded a cohort of one-celled and two-celled embryos into a room T device at 80µl/min, left them in the device for ~ 1 hour, with a trickling flow of 500nl/min and unloaded them at a rate of 300µl/min. Each embryo was then placed on an agar plate and evaluated for whether or not they had successfully developed and hatched 24 hours later. We found that the rate of hatching was 98.4% (61/62). We were thus able to optimize the parameters that ensured the viability of the embryos was not adversely affected in the microfluidic device under control conditions of uniform T.

Supplementary movies:

Movie S1

Animation of fly-over and through of device. All device sizes are approximately to scale relative to the bulk substrate of the device which has an aspect ratio of 1:3:1/25.4 (aspect ratio of a typical commercially available microscope slide)

Movie S2

High speed camera acquisition of loading of a single embryo were taken at 10k frames per second at 10x on inverted Nikon Eclipse. Replay speed was 10 frames per second.

1. Xia Y, Whitesides GM. SOFT LITHOGRAPHY. Annu Rev Mater Sci. 1998;28: 153–184. doi:10.1146/annurev.matsci.28.1.153

2. Bartolo D, Degré G, Nghe P, Studer V. Microfluidic stickers. Lab Chip. 2008;8: 274–279. doi:10.1039/b712368j

3. Wang XD, Wolfbeis OS, Meier RJ. Luminescent probes and sensors for temperature. Chem Soc Rev. 2013;42: 7834–7869. doi:10.1039/c3cs60102a

4. Ross D, Gaitan M, Locascio LE. Temperature measurement in microfluidic systems using a temperature-dependent fluorescent dye. Anal Chem. 2001;73: 4117–4123. doi:10.1021/ac010370l

5. Glawdel T, Almutairi Z, Wang S, Ren C. Photobleaching absorbed Rhodamine B to improve temperature measurements in PDMS microchannels. 2009/02/12. 2009;9: 171–174. doi:10.1039/b805172k

6. Filippov SK, Lezov A V., Sergeeva OY, Olifirenko AS, Lesnichin SB, Domnina NS, et al. Aggregation of dextran hydrophobically modified by sterically-hindered phenols in aqueous solutions: Aggregates vs. single molecules. Eur Polym J. 2008;44: 3361–3369. doi:10.1016/j.eurpolymj.2008.07.041

7. Bolker BFT, Sidles PH. Thin-film platinum resistance thermometers: Fabrication and use. J Vac Sci Technol. 1977;14: 205–209. doi:10.1116/1.569123

8. Lucchetta EM, Lee JH, Fu LA, Patel NH, Ismagilov RF. Dynamics of Drosophila embryonic patterning network perturbed in space and time using microfluidics. Nature. 2005/04/29. 2005;434: 1134–1138. doi:10.1038/nature03509

9. Johnston WL, Dennis JW. The eggshell in the C. elegans oocyte-to-embryo transition. genesis. 2012;50: 333–349. doi:10.1002/dvg.20823

10. Boggs J, Sibbitt W. Thermal Conductivity Measurements of Viscous Liquids. Ind Eng Chem. 1955;47: 53. doi:10.1021/ie50542a611

11. Hird SN, White JG. Cortical and cytoplasmic flow polarity in early embryonic cells of Caenorhabditis elegans. J Cell Biol. 1993;121: 1343–1355.

12. Bong KW, Xu J, Kim J-H, Chapin SC, Strano MS, Gleason KK, et al. Non-polydimethylsiloxane devices for oxygen-free flow lithography. Nat Commun. 2012;3: 805. doi:10.1038/ncomms1800